PHYSICAL REVIEW B VOLUME 57, NUMBER 14 1 APRIL 1998-II

Refinement of magnetic structures with x rays: Nd as a test case

D. Watson, W. J. Nuttall, and E. M. Forgan
School of Physics and Astronomy, University of Birmingham, Birmingham B15 2TT, United Kingdom

S. C. Perry
Department of Physics, Keele University, Keele, Staffordshire ST5 5BG, United Kingdom

D. Fort
School of Metallurgy and Materials, University of Birmingham, Birmingham B15 2TT, United Kingdom

(Received 5 February 1998)

We present a magnetic structural refinement using resonant magnetic x-ray scattering to investigate the antiferromagnetic structure of single-crystal elemental neodymium at 10 K. By comparison with neutron-diffraction results, we show that x rays can be used for refinement of complex magnetic structures. However, unlike neutrons, x rays distinguish between the magnetic responses of the two different Nd sites in the crystal structure. Our fits to the observed intensities are significantly improved by the inclusion of a scattering vector-dependent term reminiscent of a form factor. The theoretical issues underlying our observations are discussed. [S0163-1829(98)52214-X]

For nearly ten years the technique of resonant magnetic x-ray scattering has been applied to problems of antiferromagnetic (AF) structure.[1] Despite the experience gained, there have been few reports of magnetic structure determinations using x-ray diffraction. It is clearly of great interest to compare the capabilities of x rays and neutrons in this respect. In this paper we present a refinement of a nontrivial magnetic structure using x-ray scattering data. This follows from Detlefs and co-workers' studies which showed that magnetic x-ray scattering is sensitive to moment orientation.[2] To demonstrate and investigate the potential of the technique we have considered single-crystal elemental neodymium. This is in consequence of its complicated magnetic structure which has been well characterized using neutron and resonant magnetic x-ray diffraction.[3–9] One powerful benefit of the x-ray technique is the extremely small sample volume studied. This arises from the small incoming photon beam and its short penetration depth. Hence we can probe a single domain of magnetic structure in a high quality neodymium crystal.[9] A further benefit is the high intensity of the resonant x-ray technique (we observe AF satellites up to 3000 s^{-1} at the Nd L_{II} resonance: this represents enhancement by a factor $\sim$300 over the nonresonant signal[9]).

Neodymium has the double hexagonal-close-packed structure (dhcp), with the close-packed atomic layers in the sequence ABA′CABA′C. The layers denoted by A and A′ have a crystalline environment similar to that in a face-centered-cubic structure, whereas those labelled B and C are in approximately hexagonal-close-packed environments. Thus the two types of sites are denoted cubic and hexagonal, respectively. At 10 K, neodymium has a double-**q** sinusoidally modulated structure with the dominant magnetism being associated with the hexagonal sites. There is, however, detectable magnetization at the cubic sites where the local moments are induced by the ordered magnetization at the hexagonal sites. In the 10 K structure, the AF **q** vectors are slightly displaced from the (100) and (110) reciprocal space directions, while remaining in the basal plane, as illustrated in Fig. 1. These two **q** vectors give rise to four magnetic satellites about each reciprocal lattice point. In total we studied 96 satellites from the accessible region of reciprocal space. Such a set of Bragg reflections samples every component of the magnetic structure.

Hill and McMorrow[10] have recently described in detail the scattering amplitudes which can be used to calculate resonant magnetic intensities. They ignored, as we shall, the corrections due to point-group symmetries of the magnetic ions.[11] We note that recent observations on elemental Nd (Ref. 9) and Nd_2CuO_4 (Ref. 12) indicate the dominant transition at the L_{II} edge is electric dipole ($E1$). Synchrotron x-ray polarization is denoted conventionally by the notation σ, π for, respectively, the polarization perpendicular or parallel to the scattering plane. The scattering amplitude f_{E1}, is expressed in terms of the components of the ionic moments

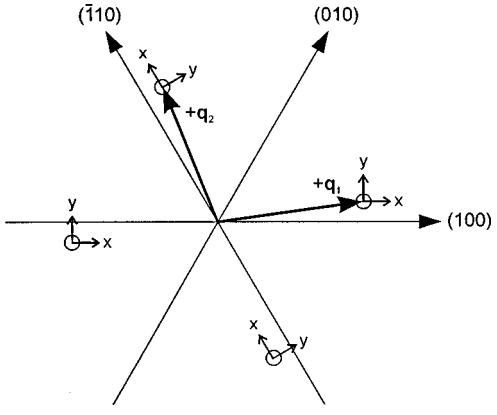

FIG. 1. Definitions of **q** vectors and Cartesian directions **x**, **y**, and **z** as used in the model for the magnetic structure. The **x** direction is the vector of direction (100) in the case of the $\mathbf{q}_1$ modulation and of direction (110) in the case of the $\mathbf{q}_2$ modulation. The **z** direction is always along (001).

resolved along the real-space Cartesian axes $\hat{\mathbf{U}}_1$, $\hat{\mathbf{U}}_2$ and $\hat{\mathbf{U}}_3$, defined[10] such that $\hat{\mathbf{U}}_2$ is perpendicular to the scattering plane and $\hat{\mathbf{U}}_3$ is along $-\boldsymbol{\kappa}$ ($\boldsymbol{\kappa}$ is the scattering vector).

We neglect terms quadratic in magnetic moment which would give rise to second-order satellites at positions $\boldsymbol{\kappa}=\boldsymbol{\tau}\pm\mathbf{q}_i\pm\mathbf{q}_j$, where i and j may be either 1 or 2. Restricting ourselves to first-order satellites of the form $\boldsymbol{\kappa}=\boldsymbol{\tau}\pm\mathbf{q}_i$, the resonant scattering amplitude matrix

$$\begin{pmatrix} f_{\sigma\sigma} & f_{\sigma\pi} \\ f_{\pi\sigma} & f_{\pi\pi} \end{pmatrix}_{E1}$$

may be expressed:

$$F^{(1)}\begin{pmatrix} 0 & -i(z_1\cos\theta+z_3\sin\theta) \\ i(z_1\cos\theta-z_3\sin\theta) & iz_2\sin 2\theta \end{pmatrix}, \tag{1}$$

where z_1, z_2, and z_3 are components along $\hat{\mathbf{U}}_1$, $\hat{\mathbf{U}}_2$, and $\hat{\mathbf{U}}_3$ of the unit vector parallel to the local moment. The constant $F^{(1)}$ is proportional to the amplitude of the local moment.[13] Since the proportionality constant has not yet been calculated theoretically we cannot use the x-ray technique to obtain the *absolute* values of the moment, but we may expect to determine the *relative* values of the moment components at a site.

We now present a way of describing the moment $\boldsymbol{\mu}^s$ at an ion site in the 10 K 2-**q** structure (s represents type of site: cubic c or hexagonal h). For each modulation vector $\mathbf{q}_i$, the moments on the two sites of a single type are related.[14] It is expected that the magnitudes of a Cartesian component β (defined in Fig. 1) of the moments will be equal[14] but may differ in phase from each other and from any other component. The individual magnetic moments $\boldsymbol{\mu}^s$ at positions $\mathbf{r}_n$ may be parameterized by two amplitudes $\mu^s_{\beta a}$ and $\mu^s_{\beta f}$ plus an overall phase α^s_β, and are given by the expression:

$$\sum_{\beta,i}\hat{\boldsymbol{\beta}}[\mu^s_{\beta f}\sin(\mathbf{q}_i\cdot\mathbf{r}_n+\alpha^s_\beta)\pm\mu^s_{\beta a}\cos(\mathbf{q}_i\cdot\mathbf{r}_n+\alpha^s_\beta)], \tag{2}$$

where the negative ambiguity corresponds to the sites A' and C and the positive ambiguity corresponds to sites A and B. If only $\mu^s_{\beta a}$ were nonzero, the moments on two sites of a given type would be exactly in antiphase. Conversely, $\mu^s_{\beta f}$ gives the in-phase component.

It is clear that the structure we have described is highly nontrivial with 12 moment components and 6 phases α^s_β to be determined by a fit to scattered intensities. Only relative phases have a meaning in an incommensurate structure such as this, so one of the phases can be set to zero (i.e., we take $\alpha^h_x=0$, for site B). In addition, for the dhcp structure it is possible to derive the relative phases of the moment components that induce moments on the other sites,[4,15] as presented in Table I. Taking the phases as fixed, the structure refinement is performed using 11 variable moments.

The diffraction measurements were made at Beamline X22-C of the National Synchrotron Light Source on two separate occasions. The single-crystal sample used was the same as that employed in our earlier x-ray studies[9] and had a mosaic spread of 0.03° full width at half maximum. It was mounted on a closed cycle refrigerator in reflection geometry with the reflecting face corresponding approximately to the (100) direction. The vertical scattering plane contained the crystal (100) and (001) directions when the diffractometer approximated to two-circle geometry. The precise orientation of the sample surface with respect to the crystal lattice (which is required to make absorption corrections) was determined by comparing the relative intensities of crystallographically equivalent reflections of $\{1\ 0\ l\}$ type. We estimated an in-plane angle of 10° between the c direction and the surface normal. Employing the instrumental four-circle capability, we were able to measure 96 satellites of the form $(0\ 0\ l)\pm\boldsymbol{\tau}'\pm\mathbf{q}_i$ where $\boldsymbol{\tau}'$ is a reciprocal lattice vector in the basal plane $\{100\}$ or (000), and l is an integer in the range 4–12. The incoming photon energy was selected to be 6.723 keV at the peak of the resonant $L_{\rm II}$ edge AF diffraction signal.

TABLE I. Relative phases of the modulated magnetic-moment components in each of the close-packed layers of the neodymium crystal structure at 10 K as inferred from the assumptions and previous observations discussed in the text.

Site	α^h_x	α^h_y	α^h_z	α^c_x	α^c_y	α^c_z
$A(c)$ or $B(h)$	0	0	$\pi/2$	0	0	$\pi/2$
$A'(c)$ or $C(h)$	π	π	$-\pi/2$	π	π	$-\pi/2$

X-ray diffraction data were collected in scans along a direction perpendicular to the Ewald sphere,[16] that is, along the direction of the short axis of the resolution ellipsoid. At large scattering angles, these scans were found to give 30% larger integrated intensities than simple rocks of the sample Bragg angle when Lorentz corrections[16] were included in the latter. All integrated intensities were corrected for absorption which is a simple function of the angles between the incident and diffracted rays and the sample surface (see, e.g., Ref. 2). Two other considerations enter into the fitting of the experimental data reported here. First, the incident beam polarization,

$$P=\frac{I_\sigma-I_\pi}{I_\sigma+I_\pi}, \tag{3}$$

was fixed at its previously reported value of 0.9 (Ref. 17). [If allowed to float, it tended towards somewhat lower values, typically 0.83(3)]. Also, for generality we have included in the amplitude a factor $\Gamma(\kappa)$ dependent on the magnitude of the scattering vector. This was taken to be a Gaussian parameterized by a length-scale r_0:

$$\Gamma(\kappa)=\exp\left[-\left(\frac{\kappa^2 r_0^2}{2}\right)\right]. \tag{4}$$

The inclusion of the term $\Gamma(\kappa)$ generated fits with a 60% lower χ^2 than if the term is set to unity. In Fig. 2 we present a comparison of our magnetic structure fit to the first data set and the observed experimental intensities. The results of our least-squares fits to both the data sets are summarized in Table II together with the results of a fit to the neutron scattering data of Lebech and coworkers.[4] The moment components are grouped into three sets: each of the components in

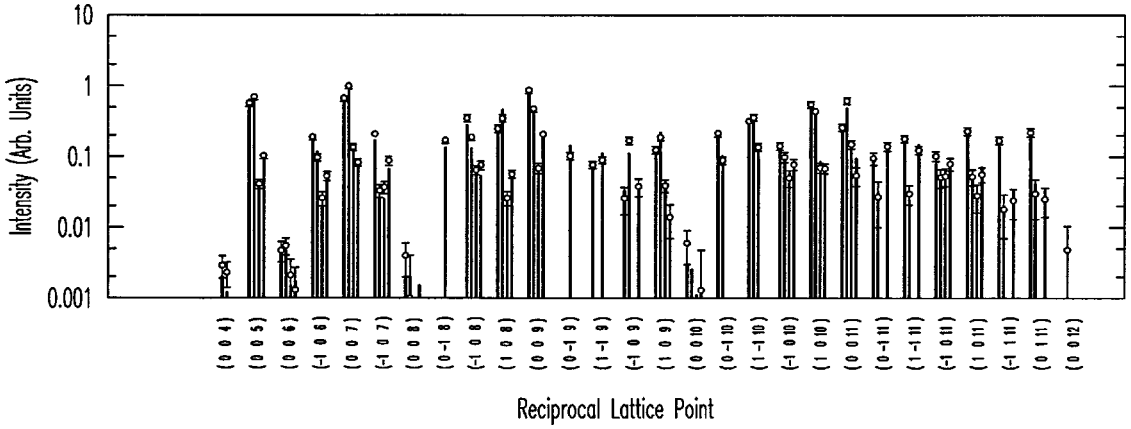

FIG. 2. Comparison of the fitted model described in the text and the experimentally determined intensities (first data set) of the x-ray magnetic satellites in the order $+\mathbf{q}_1$, $-\mathbf{q}_1$, $+\mathbf{q}_2$, $-\mathbf{q}_2$ for each reciprocal lattice point. The fitted values are represented by vertical lines and the data by circular symbols with error bars. The errors for the individual satellites are the random statistical error plus a 15% contribution due to experimental systematics.

one set induces the others,[4,15] so that they should all be present or absent together. We found no significant evidence for nonzero values of the moment components in the last set of Table II. In the final fit these were fixed at zero. We now discuss the values of the moment components. Firstly we note the excellent and reproducible agreement of the neutron and x-ray results for μ^h_{ya}. Together with μ^h_{xa}, this component defines the angle within the basal plane of the major hexagonal ordered moment; it is gratifying to show that x rays can be used to refine this angle to an accuracy of about 2°. We also note that there is agreement within errors between the two x-ray data sets and the neutron data for the magnitudes of the other hexagonal site components. However, for the components on the cubic sites, we find that the x-ray results, although consistent with one another, are approximately half those obtained with the neutron study. In this context, we note that the x-ray process involves a virtual dipole transition between the core p state and d-character states near the Fermi level. Therefore the resonant x-ray scattering is not directly measuring the $4f$ electronic moment. Instead it is measuring a magnetization ''induced'' in the d states. The different Néel transition temperatures of the hexagonal and cubic sites show that there are differing interactions of the f moments with the conduction electrons. The lower T_N of the cubic sites is consistent with the smaller magnetic x-ray response from these sites. We conclude that neutrons and x rays can give different and complementary information about magnetic structures: the latter technique is site sensitive.

TABLE II. Results of the fit to our magnetic structure model compared with the neutron-diffraction data of Ref. 4. For the first data set the ''form-factor'' parameter term $r_0 = 0.141(9)$ Å. The statistical χ^2 associated with the fit to the first data set is 2.04. For the second data set the form-factor r_0 is 0.137(13) Å. Incoming beam polarization has been fixed at the reported value of 0.9 (Ref. 17). In each case the value of μ^h_{xa} is fixed by assumption to the neutron value.

Moment	X rays(1)	X rays(2)	Neutrons
μ^h_{xa}	2	2	2.00(5)
μ^h_{xf}	0.02(2)	0.04(4)	0.06(2)
μ^c_{xf}	−0.12(2)	−0.09(5)	−0.24(2)
μ^c_{za}	−0.32(2)	−0.38(3)	−0.52(2)
μ^h_{ya}	0.47(3)	0.45(5)	0.55(3)
μ^h_{yf}	0.01(3)	0.04(6)	0.05(2)
μ^c_{yf}	0.02(3)	−0.02(7)	0.10(2)
μ^h_{za}	0	0	0
μ^h_{zf}	0	0	0
μ^c_{xa}	0	0	0
μ^c_{ya}	0	0	0
μ^c_{zf}	0	0	0

In Fig. 3 we compare the κ dependence of the intensity given by our ''form-factor'' $\Gamma(\kappa)$ with that expected from the low-temperature limit of the Debye-Waller (DW) factor for Nd (Ref. 18) and the theoretical curve for x-ray charge scattering.[19] We note that x-ray *charge* scattering falls off rapidly with κ (as does magnetic neutron scattering). However, according to the theory of resonant x-ray scattering,[20] the core excitation and de-excitation processes should depend on the *magnitudes* of the incident and scattered wave

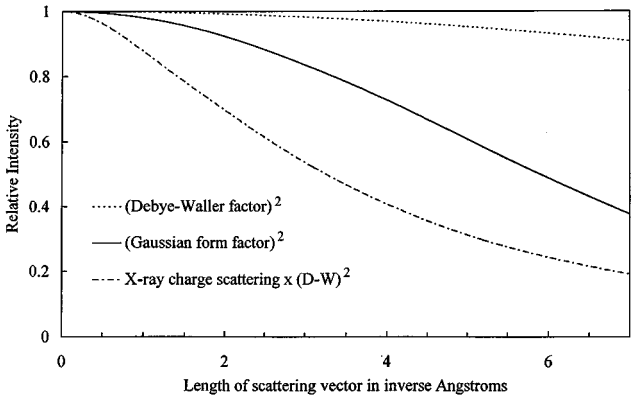

FIG. 3. Theoretical wave vector dependence of x-ray intensity expected from the zero-temperature DW factor (Ref. 18) and charge scattering (Ref. 19) (including the dispersion correction) for Nd, compared to the Gaussian model fitted to our x-ray results.

vectors, but *not* on their difference, the scattering vector κ. Hence the magnetic x-ray signal is expected to vary with κ only due to the DW factor, which is a small effect. One possible origin of the term $\Gamma(\kappa)$ is that we are failing to pick up the full scattered intensity at large scattering angles. However, in our second data set the detector slits were deliberately set larger to check for this possibility, and the similarity of the two fitted values of r_0 indicates that this effect is absent. Furthermore, we confirmed that at large angles there was no sign of any second buried AF domain within the sample. Also we are most unlikely to be missing the relevant AF domain of the crystal at these angles as the beam's footprint on the sample is smaller at larger angles. A clue to the origin of $\Gamma(\kappa)$ is given by our observations of (attenuated) charge reflections. Our data set is sparse, but we found that these fell off faster at large κ than expected for charge scattering. It may be that a *static* Debye-Waller factor due to frozen atomic disorder in the near-surface layers could explain both magnetic and charge results. Finally, we note that if $\Gamma(\kappa)$ is set to unity, the quality of our fits is reduced (the difference between data and fit tends to be positive at small κ and negative at large κ), but the relative values of the moments are essentially unaffected, so that the questions of ''form factor'' and refinement are decoupled.

In conclusion we find that it is indeed possible to use x-ray diffraction techniques for magnetic structure refinement in a similar way to neutron diffraction. This method can be used in materials such as neodymium, whose complexity has been extremely challenging even using neutron-diffraction methods. We note that there are benefits of the resonant x-ray technique, namely, high count rates, elemental specificity, site specificity, the ability to sample single magnetic domains and extremely small samples. We are confident that in particular cases x-ray scattering techniques will have much to offer the field of magnetic structure determination.

We gratefully acknowledge the assistance of D. Gibbs, W. Schoenig, S. Coburn, and others at the NSLS. We thank W. G. Stirling, J. P. Hill, M. Blume, and S. W. Lovesey for valuable discussions and B. Lebech for providing us with her neutron-diffraction data[4] which we refitted to the model of Table II. We acknowledge the financial support of the EPSRC. Work performed at the NSLS was supported by the U.S. Department of Energy under Contract No. DE-AC02-76CH00016.

[1] D. Gibbs *et al.*, Phys. Rev. Lett. **61**, 1241 (1988).
[2] C. Detlefs *et al.*, Phys. Rev. B **55**, R680 (1997).
[3] R. M. Moon, J. W. Cable, and W. C. Koehler, J. Appl. Phys. **35**, 1041 (1964).
[4] B. Lebech, J. Appl. Phys. **52**, 2019 (1981).
[5] K. A. McEwen *et al.*, Physica B&C **130**, 360 (1985).
[6] E. M. Forgan, E. P. Gibbons, K. A. McEwen, and D. Fort, Phys. Rev. Lett. **62**, 470 (1989).
[7] S. W. Zochowski, K. A. McEwen, and E. Fawcett, J. Phys.: Condens. Matter **3**, 8079 (1991).
[8] E. M. Forgan, S. L. Lee, W. G. Marshall, and D. Fort, J. Magn. Magn. Mater. **104-107**, 913 (1992).
[9] D. Watson *et al.*, Phys. Rev. B **53**, 726 (1996).
[10] J. P. Hill and D. F. McMorrow, Acta Crystallogr., Sect. A: Cryst. Phys., Diffr., Theor. Gen. Crystallogr. **52**, 236 (1996).
[11] P. Carra and B. T. Thole, Rev. Mod. Phys. **66**, 1509 (1994).
[12] J. P. Hill *et al.*, Phys. Rev. B **52**, 6575 (1995).
[13] M. Blume, in *Resonant Anomalous X-Ray Scattering*, edited by G. Materlik, C. J. Sparks, and K. Fischer (North-Holland, Amsterdam, 1994).
[14] E. M. Forgan, J. Magn. Magn. Mater. **104**, 1485 (1992).
[15] S. L. Lee, Ph.D. thesis, University of Birmingham, 1991.
[16] G. J. McIntyre and R. F. D. Stansfield, Acta Crystallogr., Sect. A: Cryst. Phys., Diffr., Theor. Gen. Crystallogr. **44**, 257 (1988).
[17] D. Gibbs *et al.*, Phys. Rev. B **43**, 5663 (1991).
[18] J. M. Ziman, *Principles of the Theory of Solids* (Cambridge University Press, Cambridge, England, 1964), p. 62.
[19] *International Tables for Crystallography*, edited by A. J. C. Wilson (Kluwer, Dordrecht, 1992), Vol. C.
[20] J. P. Hannon *et al.*, Phys. Rev. Lett. **61**, 1245 (1988).